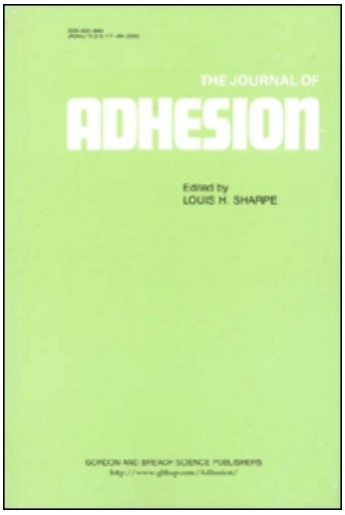

The Journal of Adhesion
Publication details, including instructions for authors and subscription information:
http://www.informaworld.com/smpp/title~content=t713453635

Aluminium-Aluminium Bonding by Rubber Blend Based on Epichlorohydrin Rubber and Carboxylated Nitrile Rubber

Tinku Bhattacharya[a]; B. K. Dhindaw[a]; S. K. De[b]
[a] Metallurgical Engineering Department, Indian Institute of Technology, Kharagpur, India [b] Rubber Technology Centre, Indian Institute of Technology, Kharagpur, India

To cite this Article Bhattacharya, Tinku , Dhindaw, B. K. and De, S. K.(1992) 'Aluminium-Aluminium Bonding by Rubber Blend Based on Epichlorohydrin Rubber and Carboxylated Nitrile Rubber', The Journal of Adhesion, 39: 4, 207 — 226
To link to this Article: DOI: 10.1080/00218469208030463
URL: http://dx.doi.org/10.1080/00218469208030463

J. Adhesion, 1992, Vol. 39, pp. 207–226
Reprints available directly from the publisher
Photocopying permitted by license only

Printed in the United States of America.

Aluminium-Aluminium Bonding by Rubber Blend Based on Epichlorohydrin Rubber and Carboxylated Nitrile Rubber

TINKU BHATTACHARYA and B. K. DHINDAW

Metallurgical Engineering Department, Indian Institute of Technology, Kharagpur 721 302, India

S. K. DE*

Rubber Technology Centre, Indian Institute of Technology, Kharagpur 721 302, India

(Received November 16, 1991; in final form June 11, 1992)

Rubber blends based on epichlorohydrin rubber and carboxylated nitrile rubber can be used as adhesives for aluminium-aluminium bonding. The bond strength depends on blend composition and moulding conditions, such as time, temperature and pressure. Lewis acid/base type interaction is responsible for this type of adhesion. The failure mechanism of the composites was studied by SEM.

KEY WORDS carboxylated nitrile rubber; epichlorohydrin rubber; aluminium-aluminium bonding; peel adhesion; failure mechanism.

INTRODUCTION

Earlier it was reported that adhesives based on carboxylated rubber and chlorinated rubber can cause metal-metal bonding.[1–8] The blend of carboxylated nitrile rubber (XNBR) and chlorobutyl rubber (CIIR) can cause aluminium-aluminium (Al-Al) bonding.[7,9] When epichlorohydrin rubber (EO) was used in place of chlorobutyl rubber (CIIR), the blend was found to act as an adhesive for Al-Al bonding. In the present communication, we report the results of our studies on the use of XNBR-EO rubber blends as adhesives for bonding of two aluminium foils.

Use of flexible Al foils enabled us to determine the adhesive strength by a 180°C peel test.[7–9] The aluminium/adhesive interface was characterized with attenuated total reflection infrared spectroscopy (ATR) and X-ray photoelectron spectroscopy (XPS).

*Corresponding author.

EXPERIMENTAL

Materials Used

The aluminium foils (thickness 0.05 mm, hardness 52.70 V.P.N.) were obtained from Indal, Bombay. Epichlorohydrin rubber (GECRHON 3100) was obtained from Nippon Zeon Co Ltd. The carboxylated nitrile rubber (XNBR) used was Krynac 231 of Polysar Ltd, Canada. In order to study the effect of the carboxyl content of XNBR on metal-metal bonding, we also used two other grades of XNBR, namely Krynac 221 and Krynac 110.

Carbon black (N-330) was obtained from Phillips Carbon Black Ltd. India.

Preparation of the Rubber Blend

Epichlorohydrin rubber (EO) was first masticated for one minute in a 35.5 cm × 15.2 cm two-roll mill. Next, XNBR was blended with EO and further masticated for 8 mins. A blend thus prepared was ready for use as a bonding agent between the metal foils. In order to characterise the blend, Mooney viscosity of both blend and neat rubbers was determined according to ASTM 1646–1963, using a Negretti Automation Mooney Shearing disc viscometer, model mk-III. In order to confirm that such a blend did not form a crosslinked structure during moulding at high temperature, we took a rheograph of the blend on a Monsanto Rheometer R-100. For the filled adhesive, carbon black filler was incorporated after blending of the two rubbers.

Preparation of the Composite

Aluminium foils were cut into 150 × 200 mm size and cleaned with acetone. 3 gm of the rubber blend was passed four times through the two-roll mill at the closest nip gap and a thin rubber layer was obtained. This rubber layer was placed between the two aluminium foils. A part of the metal foil assembly was not filled with rubber and was kept outside the mould during moulding. This part was held in the grip of the universal testing machine during peel strength testing. The dimensions of the specimen were 100 × 25 mm, while the bonded region was 50 × 25 mm. Figure 1 shows the details of the test specimen.

The following variables were considered: blend ratio, moulding time, moulding temperature, moulding pressure, carboxyl content of XNBR and carbon black filler.

Dynamic Mechanical Analysis

The loss modulus (E″) and mechanical damping (tan δ) were measured by dynamic mechanical analysis (DMA) using a Toyo Baldwin Rheovibron model DDV-III-EP at a strain amplitude of 0.0025 cm and a frequency of 3.5 Hz. The procedure was to cool the sample to −100°C and record the measurements during heating (up to room temperature) with a heating rate of 2°C/min. The glass transitions (T_g) of the

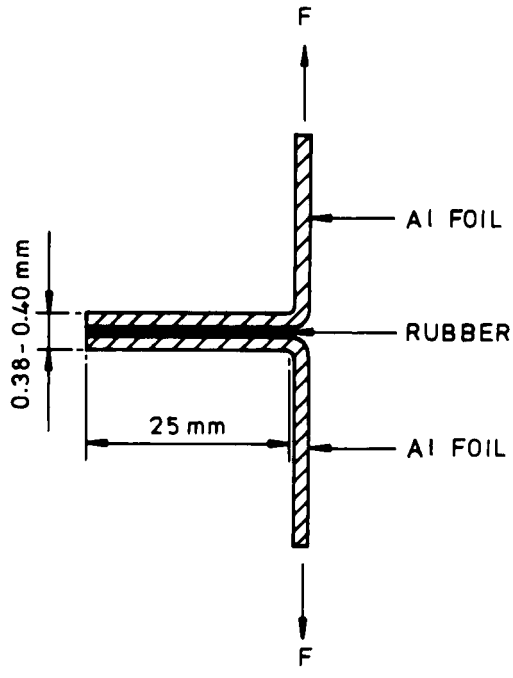

FIGURE 1 Schematic diagram of adhesive joint.

single rubbers and the blends were determined from the peak positions in the plots of loss modulus *versus* temperature and of tan δ *versus* temperature.

IR Spectroscopy

IR spectra of the individual rubbers and the blend were obtained using a Perkin-Elmer IR spectrophotometer, model 840. Thin films of rubbers were prepared by moulding at 180°C for 60 mins. Difference spectra of the blend and individual rubbers were used to examine the possible interaction occurring between individual rubbers.

Determination of 180° Peel Strength

Peel testing was done in a Zwick Universal Testing Machine (Model 1445) at a crosshead speed of 50 mm/min at room temperature.

The 180° peel strength was calculated using the following relation

$$\text{Peel strength} = 2F/w \tag{1}$$

where F = load in Newtons required to separate the layers and w = width of the specimen.

The joints were tested within two days after preparation. The results were found to vary within ±5%.

Scanning Electron Microscopic Study

After peeling, test specimens were sputter coated with gold within 24 h of peeling and studied microscopically using a Camscan SEM, series 2DV. The areas scanned included the peel front, the metal-rubber interface and the peeled adhesive surface.

ATR and XPS Analysis

0.2 gm of masticated rubbers of XNBR, EO and the blend were placed between 10 cm × 10 cm aluminium foils and moulded for 60 mins at 180°C, under a moulding pressure of 0.69 MPa. Care was taken during mill mixing to avoid contamination. These composites were made to fail by peeling in the Zwick machine. The interface was repeatedly (four times) exposed in chloroform to remove the unreacted blend.[10] It is believed that such solvent extraction leaves only bound adhesive at the interface. Excess chloroform was removed by evacuation in a vacuum oven for 48 h. The leached surface was used for ATR and XPS analyses.

XPS was done using an ESCA LAB II VG Scientific Ltd. instrument, with a magnesium anode (12 KV). All samples were scanned from 0 to 1100 ev. Argon ion sputtering was done in order to study the chemical composition of the interface.

ATR spectra were obtained with a SHIMADZU IR-470 spectrophotometer using an ATR-2A, multiple reflection type attenuated reflectance attachment. A KRS-5 (thallium bromoiodide) crystal, an internal reflection accessory, was used at an angle of 45° to obtain the ATR spectra. A section 2 cm × 2 cm long was cut from the failure surface and the leached surface was analyzed by ATR.

RESULTS AND DISCUSSION

Mooney viscosity values of epichlorohydrin (EO), carboxylated nitrile rubber (XNBR) and the 1:1 blend were 20, 30 and 15 respectively. Low viscosity of the blend ensures its free flow while placed between two aluminium foils prior to moulding.

DMA studies showed that the blend was miscible at the segmental level at all blend ratios (Table I and Fig. 2). A single peak, occurring between the T_g's of the individual rubbers, was obtained for all blend ratios.

Figure 3 shows the Monsanto rheographs of the 1:1 blend of EO and XNBR and the individual rubbers over a period of two hours at 180°C. Constancy in rheometer torque of the blend indicates that no crosslinking takes place between EO and XNBR. The rheograph of EO shows that degradation takes place only after 20 mins, whereas XNBR alone and the blend are thermally stable at 180°C up to 120 mins.

Further evidence of the absence of self-crosslinking between the two rubbers in the blend was proved by solubility studies and IR analysis. Single rubbers, as well as the blend, after heat treatment at 180°C for 60 mins, were soluble in chloroform.

TABLE I
Glass transition temperature (T_g) from dynamic mechanical analysis

Sample	T_g(°C)	
	Mechanical damping (tan δ)	Loss modulus (E″)
EO	−31.25	−40.00
EO:XNBR Blend 1:1	−21.25	−29.37
XNBR	−13.30	−21.25

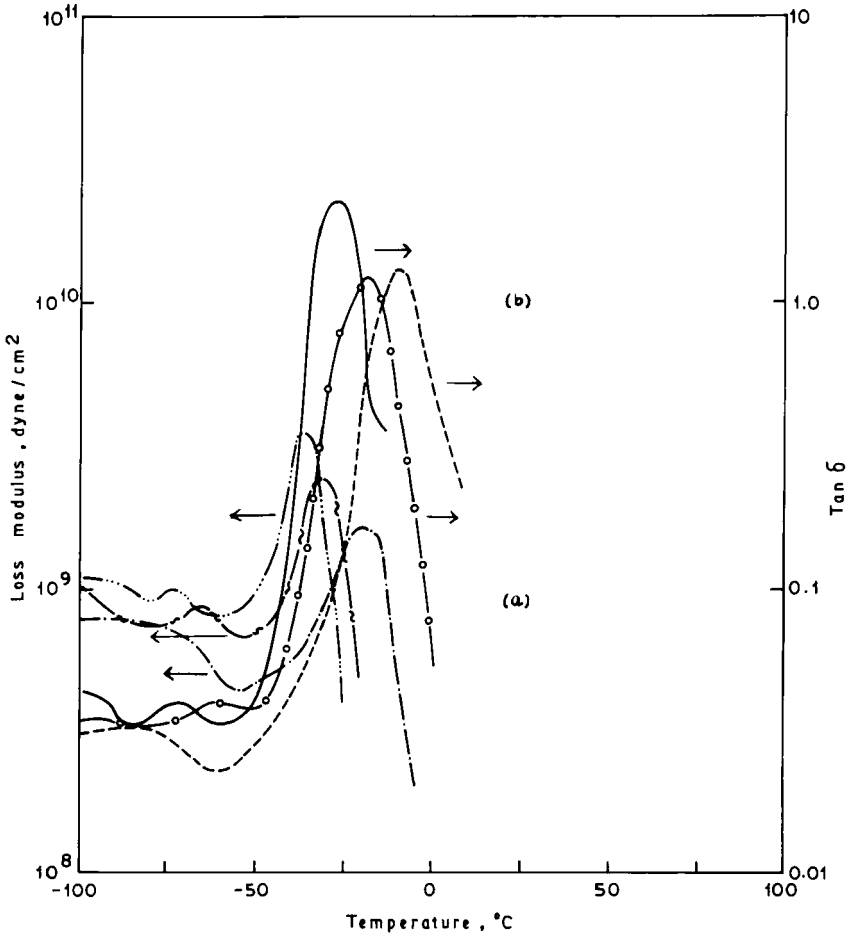

FIGURE 2 Plots of loss modulus and tan δ *versus* temperature for individual rubbers and the 1:1 blend. (a) Loss modulus *vs.* temperature —·····— Eo —·—·— XNBR —~—~— Blend; (b) Tan δ *vs.* temperature —— EO --- XNBR —○— Blend

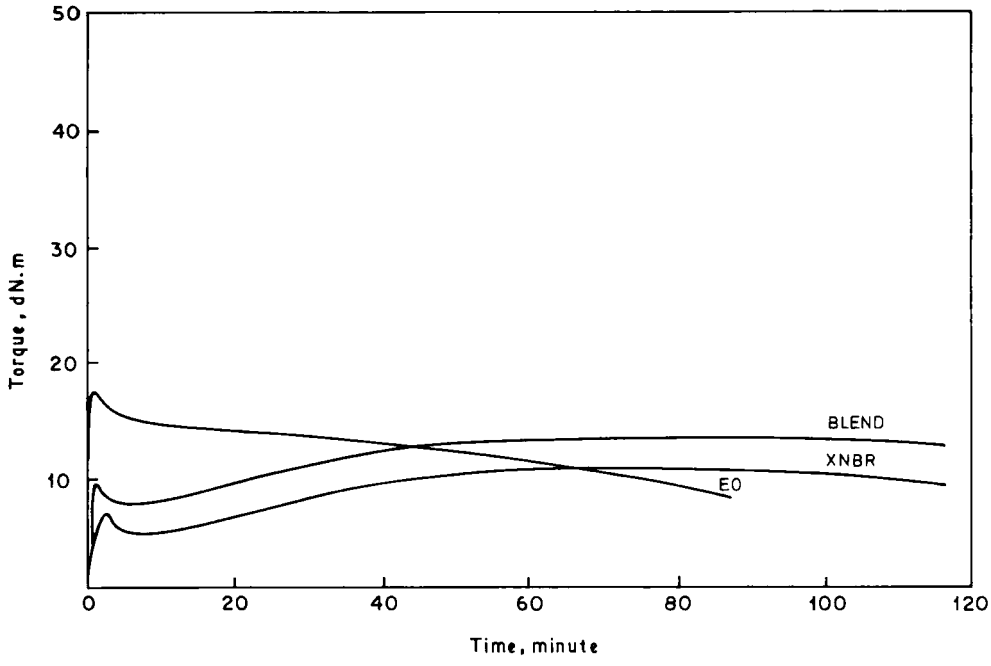

FIGURE 3 Monsanto rheograph of EO, XNBR and 1:1 blend of EO and XNBR at 180°C.

Figure 4a represents the difference spectrum of the blend and XNBR. The negative peaks at 1735 cm^{-1} are due to the stretching mode of free CO_2H and the band at 1669 cm^{-1} appears from the antisymmetric C=O stretching mode in a hydrogen bonded CO_2H group. These peaks are due to XNBR itself. This shows that the CO_2H group in XNBR exists predominantly in the hydrogen bonded form. The C—Cl stretching vibration comes at 746 cm^{-1}, which is due to epichlorohydrin (Fig. 4b). Similarly, the difference spectrum of the blend and epichlorohydrin shows that the C=O peak appears at 1736 cm^{-1} due to the free CO_2H group and a small band around 1700 cm^{-1} indicates a minor fraction of hydrogen-bonded acid. The above results also prove that no chemical reaction has taken place between EO and XNBR.

Effect of Blend Ratio

Single rubbers did not cause Al-Al bonding and, in both cases, we noted rubber-metal failure (Tables II and III). The blend of EO and XNBR, however, caused Al-Al bonding and the degree of bonding, as measured by peel strength, was found to depend upon blend ratio. The largest peel strength was obtained at an EO and XNBR blend ratio of 1:3 (Table IV).

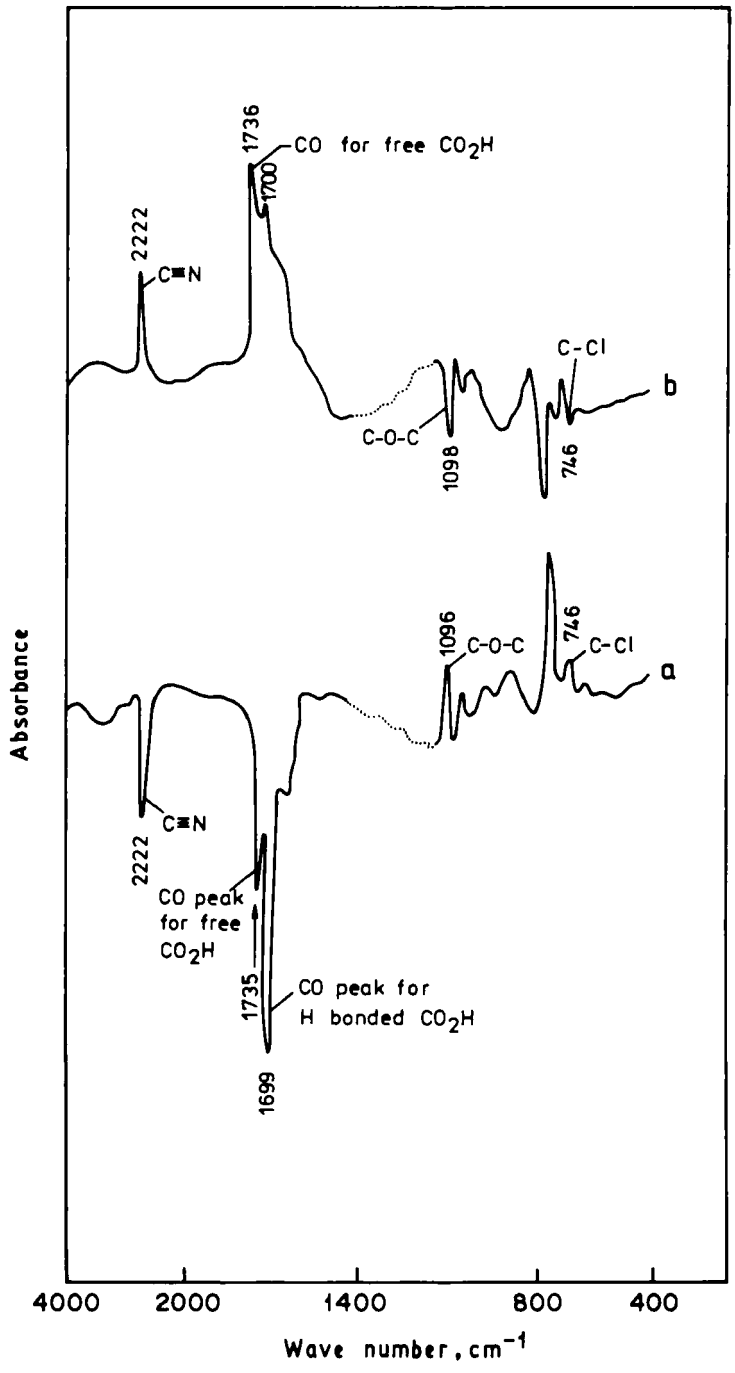

FIGURE 4 (a) Difference IR spectrum of the blend and carboxylated nitrile rubber. (b) Difference IR spectrum of the blend and epichlorohydrin rubber.

TABLE II
Dependence of peel strength of Al-Al joints bonded by epichlorohydrin and carboxylated nitrile rubbers on moulding temperature

Rubber	Moulding temperature (°C)	Peel strength[a] (N/m)	Mode of failure
EO	160	160	Rubber-metal
XNBR	160	0	Rubber-metal
EO	170	240	Rubber-metal
XNBR	170	0	Rubber-metal
EO	180	1,280	Rubber-metal
XNBR	180	0	Rubber-metal
EO	190	1,600	Rubber-metal
XNBR	190	0	Rubber-metal

[a]Moulding time 60 min; moulding pressure 0.35 MPa in all cases.

TABLE III
Dependence of peel strength of Al-Al joints bonded by epichlorohydrin and carboxylated nitrile rubbers on moulding pressure

Rubber	Moulding pressure (MPa)	Peel strength[a] (N/m)	Mode of failure
EO	0.17	2,000	Rubber-metal
XNBR	0.17	0	Rubber-metal
EO	0.35	1,280	Rubber-metal
XNBR	0.35	0	Rubber-metal
EO	0.69	1,040	Rubber-metal
XNBR	0.69	0	Rubber-metal

[a]Moulding time 60 min; moulding temperature 180°C.

Effect of Moulding Time

At 180°C, the composites were moulded for different times, under a constant pressure of 0.35 MPa. The results are summarized in Table V. The peel strength increased with increasing moulding time, reaching a plateau at approximately 90°C (Fig. 5). In all cases, peel failure was of the cohesive (rubber-rubber) type. With increase in moulding time adhesive flow increases, wettability increases, resulting in an increase in peel strength. Smoothness of the failure surface indicates an increase in wettability with moulding time.[7,8] At low moulding time, non-uniform cohesive failure took place due to restricted flow and the peeled adhesive surface was rough. When moulding time was increased to 60 mins, peel strength increased due to better wetting, resulting in cohesive failure with a smooth surface.

Reusability of the Adhesive

The EO:XNBR blend can be useful as a reusable laminating adhesive. Its reusability as a dry adhesive was tested by moulding the peeled samples at 180°C for a second time. The results are tabulated in Table VI. At low moulding time, the peel

TABLE IV
Dependence of peel strength on blend ratio

Blend ratio XNBR:EO	Peel strength[a] (N/m)	Mode of failure
1:3	6,000	Rubber-rubber
1:1	9,040	Rubber-rubber
3:1	10,000	Rubber-rubber

Moulding temperature 180°C; moulding pressure 0.35 MPa; moulding time 60 min.

TABLE V
Dependence of peel strength on moulding time[a]

Moulding time (min)	Peel strength (N/m)	Mode of failure
5	4,000	Non-uniform rubber-rubber
30	6,400	Non-uniform rubber-rubber
60	9,040	Uniform rubber-rubber
90	9,760	Uniform rubber-rubber
120	9,600	Uniform rubber-rubber

[a]1:1 EO:XNBR blend; moulding temperature 180°C; moulding pressure 0.35 MPa.

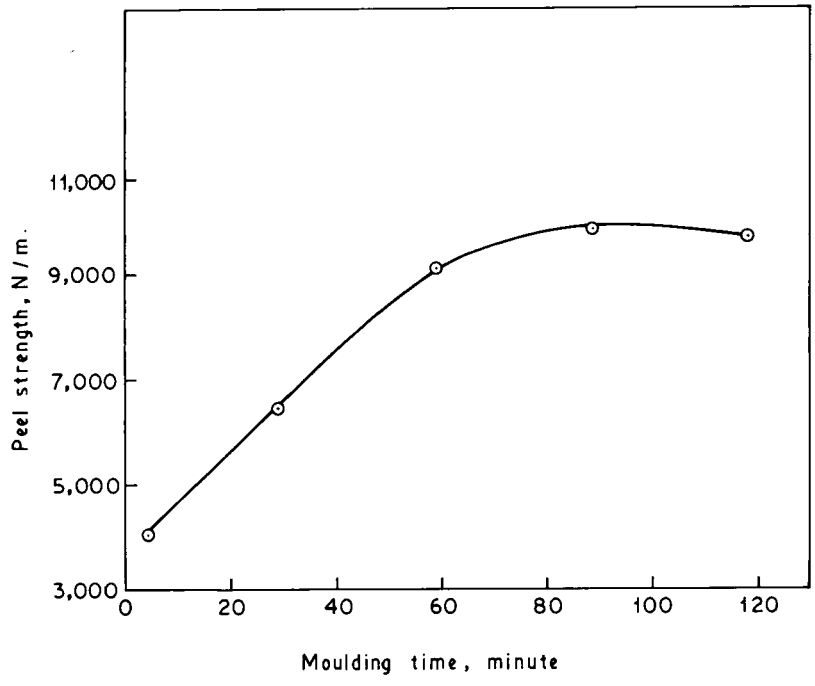

FIGURE 5 Dependence of peel strength on moulding time.

TABLE VI
Dependence of peel strength on post-peel moulding[a]

Moulding time (min)	No. of peel[b]	Peel strength (N/m)	Mode of failure
5	1	4,000	Non-uniform rubber-rubber
	2	3,520	Non-uniform rubber-rubber
30	1	6,400	Non-uniform rubber-rubber
	2	6,880	Non-uniform rubber-rubber
60	1	9,040	Uniform rubber-rubber
	2	6,080	Combination of rubber-rubber and rubber-metal
90	1	9,760	Uniform rubber-rubber
	2	5,120	Rubber-metal

[a]1:1 EO:XNBR blend; moulding temperature 180°C; moulding pressure 0.35 MPa
[b]1. means original moulding; 2. means second time moulding after first peel.

strength remained unchanged when the samples were moulded for the second time. However, at high moulding time the strength decreased after the second moulding. This occurred because the second moulding caused flow-out of the adhesive from the laminate causing a decrease in the adhesive content. Since the adhesive was uncrosslinked, and no mould was used to contain it, flow-out under pressure during moulding at high temperature was facilitated. The second moulding would, therefore, cause further loss of adhesive from the composite.

Effect of Moulding Temperature

At a moulding pressure of 0.35 MPa, the adhesive joints containing the above blend were moulded for 60 mins at different temperatures. It is evident from Table VII that with an increase in moulding temperature joint strength increased, reached a maximum at 180°C, and then dropped. At moulding temperatures of 180°C and below, the mode of failure was cohesive (rubber-rubber). The peeled surface was uniform on both surfaces of the metal. At 190°C moulding temperature the mode of failure changed to interfacial (rubber-to-metal), with a reduction in peel strength.

Effect of Moulding Pressure

The peel strength was found to depend on moulding pressure (Table VIII). With increase of moulding pressure, peel strength decreased due to decrease of adhesive

TABLE VII
Dependence of peel strength on moulding temperature[a]

Moulding temperature (°C)	Peel strength (N/m)	Mode of failure
160	5,680	Rubber-metal
170	6,480	Rubber-metal
180	9,040	Rubber-rubber
190	6,320	Initially rubber-rubber followed by rubber-metal

[a]1:1 EO:XNBR blend; moulding pressure 0.35 MPa; moulding time 60 min.

TABLE VIII
Dependence of peel strength on moulding pressure[a]

Moulding pressure (MPa)	Peel strength (N/m)	Mode of failure
0.69	7,280	Rubber-metal
0.35	9,040	Rubber-rubber
0.17	9,600	Rubber-rubber

[a]1:1 EO:XNBR; moulding temperature 180°C; moulding time 60 min.

film thickness. At a pressure of 0.69 MPa, peel strength was low due to reduced thickness of the adhesive layer and the failure mode was interfacial (rubber-to-metal) in nature. With increase of adhesive film thickness (or decrease in moulding pressure) peel strength increased, indicating that more energy is dissipated in the larger volume of adhesive.

Effect of Carboxyl Content of XNBR

Carboxyl content of XNBR was found to have a profound influence on peel strength (Table IX). Krynac 231 and 221, with high carboxyl content, showed cohesive (rubber-rubber) failure, whereas Krynac 110 with low $—CO_2H$ content showed interfacial (metal-rubber) failure. It is evident that increase in the $—CO_2H$ content of XNBR causes increase in peel strength.

Effect of Filler Loading

The influence of carbon black filler on the peel strength of the composite is shown in Figure 6. The composites were moulded for various times at 180°C, under a moulding pressure of 0.35 MPa.

The strength of carbon black filled adhesive joints was remarkably improved compared with the gum compound, because of the reinforcing effect of the black. For the 10 phr carbon black loaded system, peel strength increased with moulding time, but higher moulding time (120 min) caused interfacial failure. The failure surface was found to be smooth and uniform. However, the peel strength decreased for the 20 phr filler loaded system. Presumably, this occurs because high filler

TABLE IX
Dependence of peel strength on carboxyl content of XNBR[a]

Grade of XNBR	Absorbance ratio between C=O and C=N (determined IR spectroscopy)	Peel strength (N/m)	Mode of failure
110	0.38	1,680	Rubber-metal
221	3.30	8,480	Rubber-rubber
231	3.32	9,040	Rubber-rubber

[a]1:1 EO:XNBR blend; moulding temperature, 180°C; moulding pressure 0.35 MPa.

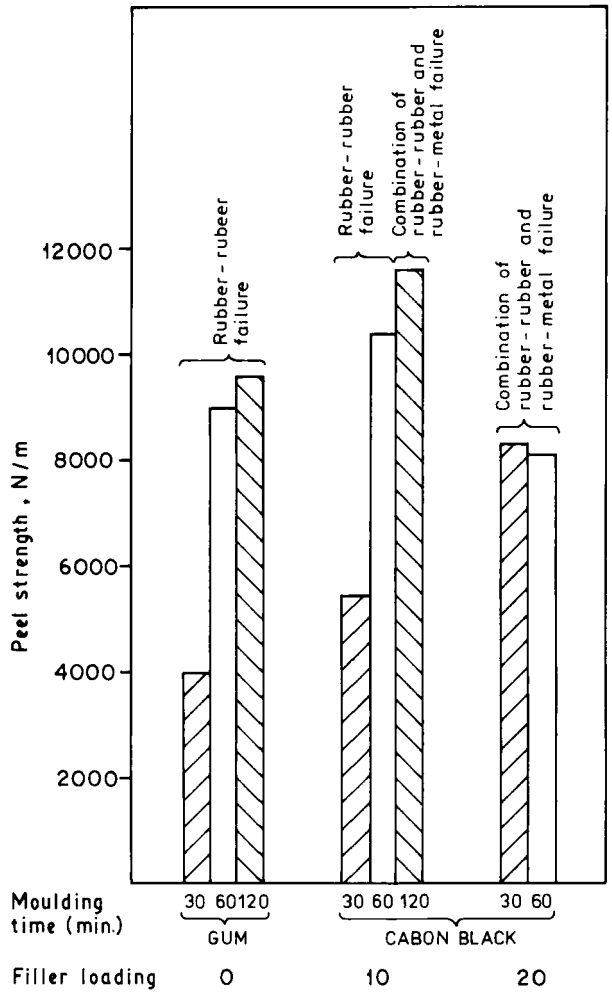

FIGURE 6 Dependence of peel strength on filler loading.

loading reduces viscoelasticity, restricts the chain mobility and reduces the interfacial strength.[11]

Scanning Electron Microscopic Study

The adhesive/aluminium interface, peel front and failure surface were examined by SEM in order to investigate the peel failure mechanism. Figure 7 shows the aluminium/adhesive interface. Because of good wetting by the adhesive, no boundary is visible between the rubber and the metal, only a diffuse interface.

Figure 8 shows a crack line in the peel front of the adhesive system during peeling, indicating an apparent brittle fracture. However, the scanning electron photomicrograph (Fig. 9) at higher magnification, with the instrument in the derivative mode,

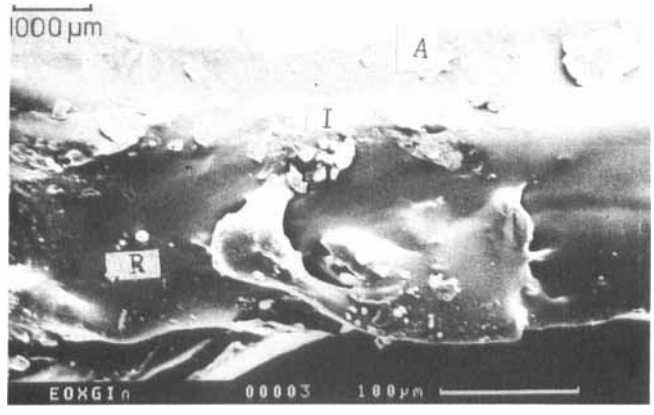

FIGURE 7 SEM photomicrograph showing metal-rubber interface. (R, Rubber; I, Interface; A, Aluminium).

shows that inside the crack a rubber layer remained on the metal. It seems that the cracks developed due to inherent weakness in the adhesive system. Again the peeled surface shows a "river" pattern (Fig. 10) which is characteristic of ductile fracture.[12–14] Moreover, the appearance of the river pattern on the surface implies that the failure, although cohesive in nature, occurred more easily and possibly under low strain, since there is no crosslinking in the adhesive layer.

The carbon black filled composite shows an almost similar pattern of fracture to that of the unfilled adhesive system. Besides the crack line, voids were also observed. As the peeling progresses, these voids grow, coalesce and cause separation (Figs. 11–12). This is due to increase in the strength of adhesive interlayer by the carbon black reinforcement which is evident from the increased strength of the

FIGURE 8 SEM photomicrograph showing peel front for gum adhesive. (C, Crack; R, Rubber).

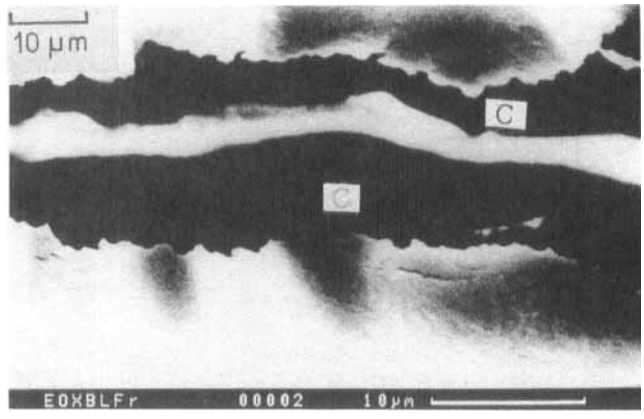

FIGURE 9 SEM photomicrograph showing magnified view of the inside crack, as shown in Fig. 8. (R, Rubber; C, Crack).

rubber adhesive. Figure 13 shows a crack far removed from the peel front. A magnified view of the crack (Fig. 14), with the instrument in the derivative mode, shows that the fissures occur due to possible gas entrapment, *e.g.*, moisture.

XPS Analysis

The interaction of the Al surface with the adhesive film was characterized with XPS by monitoring the energy of the core electrons. In Figure 15 Al2p, C1s, O1s and N1s photopeaks are shown for the Al surface from which the gum adhesive had been leached, before and after argon ion etching. The photopeaks for the neat Al foil are also shown in the same figure for comparison. The XPS results are explained in the following way.

FIGURE 10 SEM photomicrograph showing cohesively-failed peeled rubber surface for gum adhesive, the peel front of which is shown in Fig. 8. (R, Rubber).

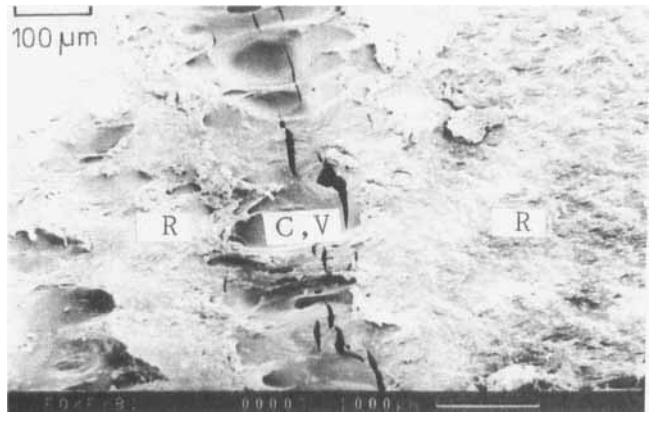

FIGURE 11 SEM photomicrograph showing peel front for carbon black filled adhesive. (R, Rubber; C, V, Cracks and Voids on peel front).

Aluminium foil: The XPS results show that the Al surface was contaminated, because no peak for Al was observed before argon ion sputtering. After argon ion sputtering for 5 mins, the following three peaks were clearly observed: Al2p at 75.7 ev, C1s at 285 ev and 01s at 533.3 ev. This indicates the possibility that Al_2O_3 is present on the Al foil.

Aluminium surface from which gum adhesive was leached: Before argon ion sputtering two peaks, C1s and O1s, were observed. But after argon ion sputtering for 10 min two peaks, *i.e.* C1s at 285 ev and N1s at 401 ev, were observed. No Al2p peak was observed even after 10 mins etching, when the O1s peak disappears. These results show that the adhesive interlayer penetrates into the pores of the Al surface and cannot be removed by solvent leaching. The C1s photopeak shows the presence of methylene carbon. This is probably due to contaminants from the surroundings.

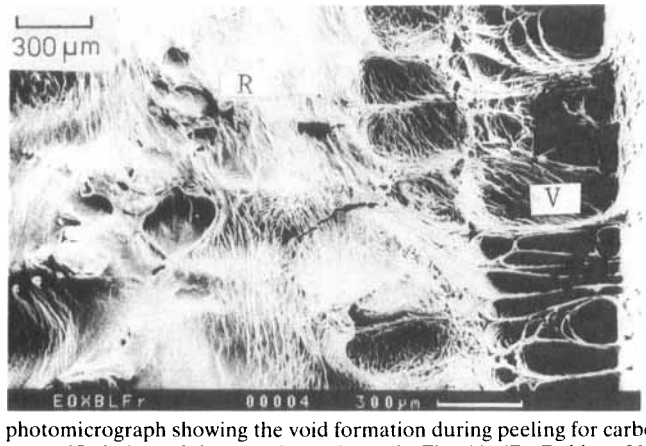

FIGURE 12 SEM photomicrograph showing the void formation during peeling for carbon-black-filled adhesive. This is the magnified view of the peel front shown in Fig. 11. (R, Rubber; V, Voids).

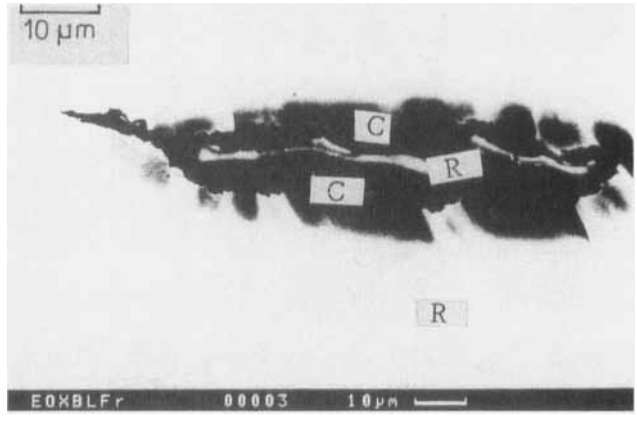

FIGURE 13 SEM photomicrograph showing a crack, in the rubber phase far removed from the peel front. This is the magnified view of the rubber phase shown in Fig. 11. (C, Crack; R, Rubber).

ATR Analysis

ATR is an important technique for investigation of the molecular structure of an adhesive/adherend interface.[15,16] Fig. 16a shows the ATR spectrum of the peeled adhesive surface, when XNBR alone was used as the adhesive. Fig. 16b is the spectrum of leached aluminium surface. Fig. 16c is the difference spectrum between XNBR on the Al surface and the leached Al surface. It shows that the XNBR does not react with the aluminium foil. Fig. 16d shows the ATR spectrum of the peeled adhesive surface when EO was used as the adhesive. Fig. 16e is the spectrum of the leached Al surface and Fig. 16f is the difference spectrum between EO on Al and the leached Al surface. This also shows that no reaction takes place between EO and the Al foil.

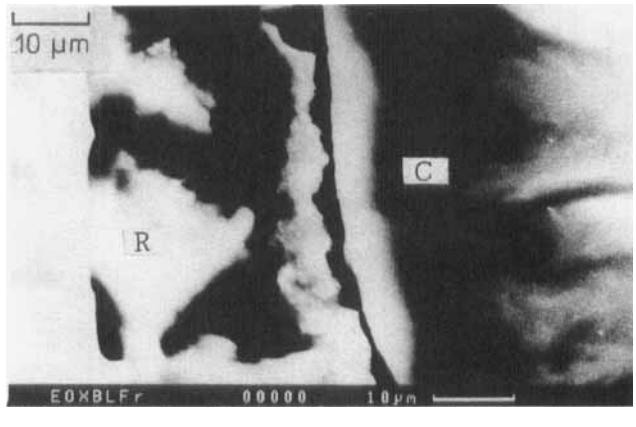

FIGURE 14 SEM photomicrograph showing magnified view of the crack in the peel front as shown in Fig. 11. (R, Rubber; C, Crack).

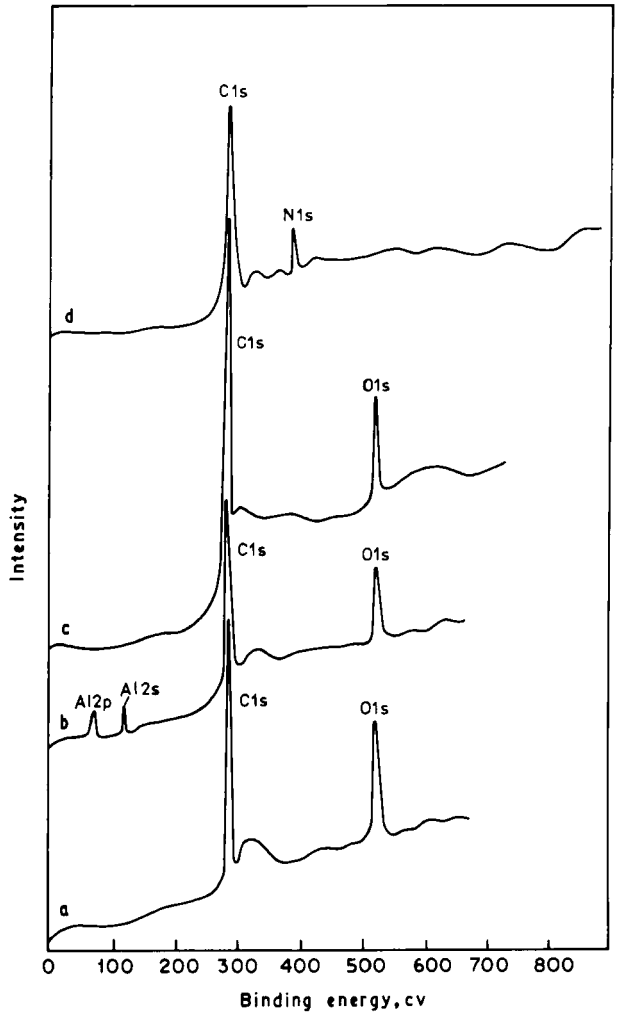

FIGURE 15 X-ray photoelectron spectra of the aluminium foil and the aluminium surface from which the gum adhesive had been leached. a) aluminium foil before etching; b) aluminium foil after etching; c) leached aluminium surface from which the gum adhesive has been leached. Before argon etching; d) same as c) but after argon etching

Figs. 16 (g, h, k) show the ATR spectrum of the XNBR-EO blend on Al foil, the leached Al surface, and the difference spectrum between the two. A new peak at 1728 cm^{-1} was observed which can be ascribed to carbonyl involved in H-bonding with surface AlOH groups or with O—Al—O groups.[17]

Fig. 17a shows the difference spectrum between the rubber blend on Al foil and EO on Al foil. A new peak at 1728 cm^{-1} was observed, presumably due to interactions between the $—CO_2H$ group of the blend and the Al surface. Fig. 17b represents the difference spectrum between the blend on Al foil and XNBR on Al foil.

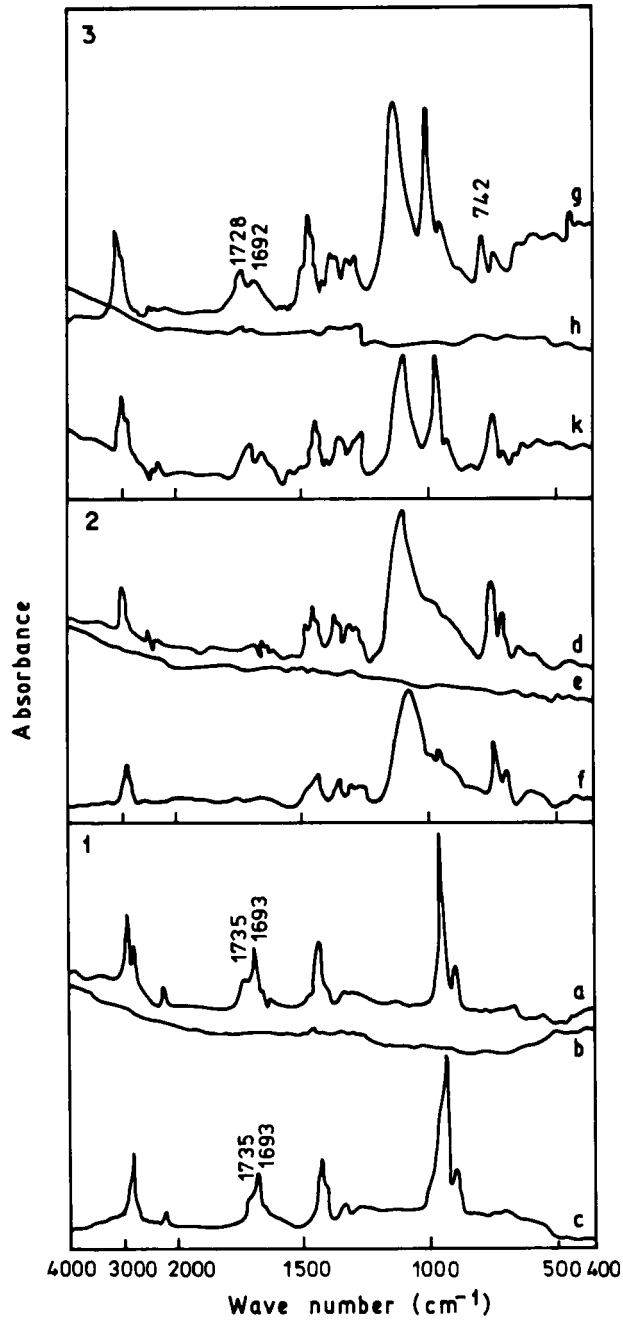

FIGURE 16 ATR spectra; a) carboxylated nitrile rubber adhesive (XNBR) on aluminium foil; b) leached aluminium surface; c) difference spectrum between XNBR on aluminium foil and leached aluminium surface; d) epichlorohydrin rubber adhesive on aluminium foil; e) leached aluminium surface; f) difference spectrum between EO on aluminium foil and leached aluminium surface; g) rubber blend on foil; h) leached aluminium surface; k) difference spectrum between rubber blend on aluminium foil and leached aluminium surface.

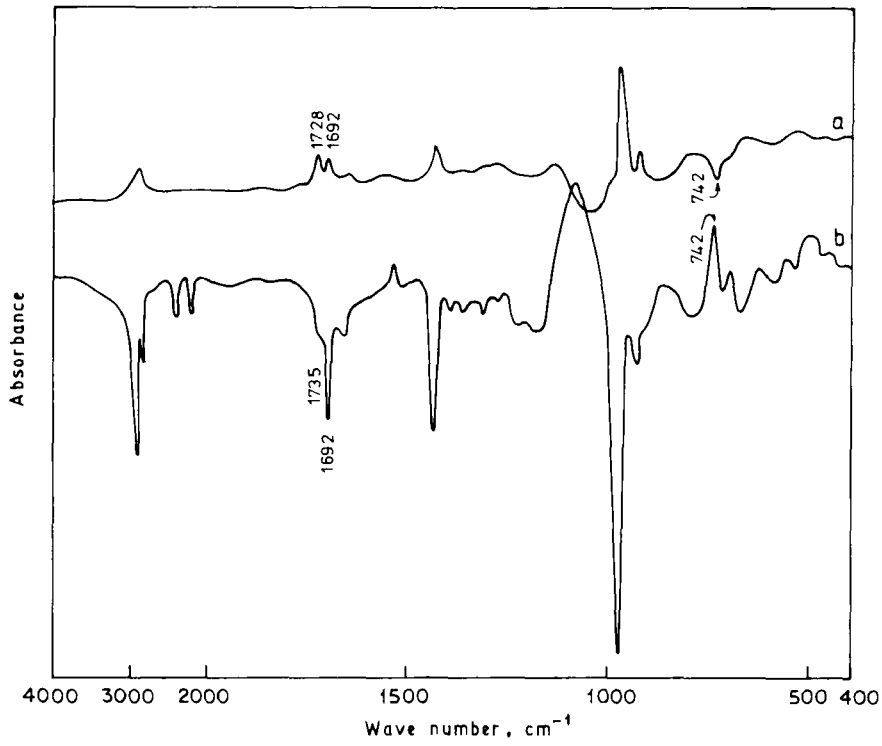

FIGURE 17 (a) Difference spectrum between rubber blend on aluminium foil and epichlorohydrin rubber on aluminium foil. (b) Difference spectrum between rubber blend on aluminium foil and carboxylated nitrile rubber on aluminium foil.

The negative peak at 1693 cm^{-1} is presumed due to hydrogen bonded —CO_2H from XNBR.

It is apparent that an interaction between the adhesive and the adherend occurs *via* the —CO_2H group. Al_2O_3 can act as Lewis donor.[18–20] The carboxylic acid group is considered to be a Lewis acid but in XNBR it remains mainly in the hydrogen bonded form, as is evident from the IR spectrum. This hydrogen bonded carboxyl oxygen might well act as an electron donor similar to the ester groups and act as a Lewis base. This is presumably why no bonding has taken place between XNBR and the Al adherend. However, when the EO and XNBR are blended together and moulded for one hour at 180°, the blend bonds well with Al. It is assumed that, in the blend, the acidity of the OH group increases due to the —Cl group and that the CO_2H can then interact with the Al surface.

CONCLUSIONS

A blend of epichlorohydrin rubber and carboxylated nitrile rubber (XNBR) can be used for Al-Al bonding. The adhesive was found to be reusable. The blend ratio,

moulding conditions and carboxyl content of the XNBR can affect the peel strength. The Lewis/acid base interaction between Al foil and the adhesive are probably the cause of this bonding.

Acknowledgment

The authors are thankful to Miss Alka Thakur of this Institute for assistance with the ATR scans.

References

1. *Handbook of Adhesives*, I. Skeist, Ed. (Van Nostrand Reinhold, New York, 1990).
2. H. P. Brown and J. F. Anderson, *Nitrile Rubber Adhesives* (Reinhold Publishing, New York, 1962), p. 220.
3. F. M. Rosenhulm, *Adhesives Age*, **22,** 19 (1979).
4. H. P. Brown, *Rubber Chem. Technol.*, **30,** 1347 (1947).
5. H. Burrell, *J. Paint Technol.*, **40,** 197 (1968).
6. D. A. Peterson, *Adhesives Age*, **12,** 25 (1969).
7. Tinku Bhattacharya, B. K. Dhindaw and S. K. De, *J. Adhesion*, **34,** 45 (1991).
8. Susy Vaghese, D. K. Tripathy and S. K. De, *J. Adhesion Sci. Technol.*, **4,** 847 (1990).
9. Tinku Bhattacharya, B. K. Dhindaw and S. K. De, *J. Adhesion Sci. Technol.* (in press).
10. W. J. van Ooij, T. H. Visser and M. E. F. Briemond, *Surf. Interf. Anal.* **6,** 197 (1984).
11. Anil Bhowmick, P. Loha and S. N. Chakrabarty *Int. J. Adhesion and Adhesives*, **9,** 2 (1989).
12. K. J. Kim, C. J. Nelson, L. E. Vescelius and G. A. Bohm, *Scanning Electron Microscopy*, **11,** 533 (1982).
13. P. K. Pal and S. K. De, *Rubber Chem. Technol.*, **55,** 1370 (1982).
14. Jossit Kurian, G. B. Nando and S. K. De, *J. Adhesion*, **20,** 293 (1987).
15. A. Garton, *Polym. Composites*, **5,** 258 (1984).
16. A. Garton, *J. Polym. Sci., Polym. Chem. Ed*, **22,** 1495 (1984).
17. Laila Uleren and Thomas Hjertberg, *J. Adhesion*, **31,** 117 (1990).
18. F. M. Fowkes, D. O. Tischer, J. A. Wolfe, L. A. Lannigau, C. M. Ademu-Jhon and M. J. Halliwal, *J. Polym. Sci., Polym. Chem. Ed*, **22,** 547 (1984).
19. F. M. Fowkes, in *Physico-Chemico Aspects of Polymer Surfaces*, Vol 2, K. L. Mittal Ed. (Plenum Press, New York, 1983), p. 583.
20. J. Schultz, L. Lavielle, *Makromol, Chem., Makromol. Sympos.*, **23,** 343 (1989).
21. L. J. Bellamy, *The Infrared Spectra of Complex Molecules*, Vol 2, 2nd Ed. (Chapman and Hall, London, 1980), p. 156.
22. D. J. Ondrus, F. J. Boerio, and K. J. Grannen, *J. Adhesion*, **29,** 27 (1989).
23. J. Schultz, L. Lavielle, A. Carre, and P. Comien, *J. Mat. Sci.*, **24,** 4363 (1989).
24. D. Briggs, in *Practical Surface Analysis by Auger and X-ray Photoelectron Spectroscopy*, D. Briggs and M. P. Seah, Eds. (John Wiley & Sons Ltd, New York, 1983), p. 359.
25. C. U. Ko, E. Bacells, T. C. Ward and J. P. Wightman, *J. Adhesion*, **28,** 247 (1989).
26. A. Holmstron and E. M. Sorvick *J. Appl. Polym. Sci.*, **18,** 761 (1974).